Lecture 13 (10-22-83)
22 October 1983

SATELLITE OBSERVATIONS OF THE OCEAN:

I. Introduction

A. Of interest not only to oceanography and ocean activities, but to meteorology; important in longer range forecasting + climate studies. Will not cover ice here; it was covered in lecture 11.

B. Will cover the following: Sea surface temperature, surface winds over the oceans, significant wave height, ocean currents and bottom topography, images by synthetic aperture radar, ocean color observations (for chlorophyll, sediment + some pollution detection).

II. Sea surface temperature.

A. Qualitative indication of gradients using NOAA AVHRR IR.

✓ – Figure 13-1 (slide): Enhanced image of SST for Gulf Stream analysis. Temperature gradients indicate current boundaries.

✓ – Figure 13-2 (slide): Analysis of above, May 1-4, 1977.

✓ – Figure 13-3 (slide): Enhanced image upwelling-produced "fronts" off the US West Coast. (11 Sept. 1974) Used by fishermen.

B. Quantitative determination from NOAA AVHRR. Done world-wide using 4 km GAC data, corrected for atmosphere using TOVS. Data processed to 1.0° (daily + weekly) and 5.0° (daily, weekly, monthly) degree lat.-long. grids. U.S. coastal waters are mapped to 0.5° resolution.

✓ – Figure 13-4 (slide): AVHRR 4 vs. 5 channel algorithms. Discuss effect of El Chichon volcano; Noisy 3.8 μm window channel (NOAA-7); NOAA-8 has 4 Ch AVHRR

✓ – Figure 13-5 (slide): Shows difference in SST mapping "noise", old vs. new algorithm Oct. vs. Nov. 81; operational switch-over was Nov. 10.
A. Strong gives figures for SST comparison (compared to buoys) from Nov. 81 thru July 82 {BIAS -0.22 °C, RMS 0.68}

C. Use of GOES

✓ – Figure 13-6 (slide): Cloud filtering by using ~~48~~ IR images in 24 hours; shows the Loop current in Gulf of Mexico. (accuracy not as good as AVHRR.)

✓ – Figure 13-7 (slide): Using VAS 3.9, 11 & 12.7 μm channels (similar to AVHRR, but lower resolution); cloud filtering by series of VAS "images".

Fig. 13-1 Sea Surface Temperature - Enhanced Image of SST for Gulf Stream Analysis

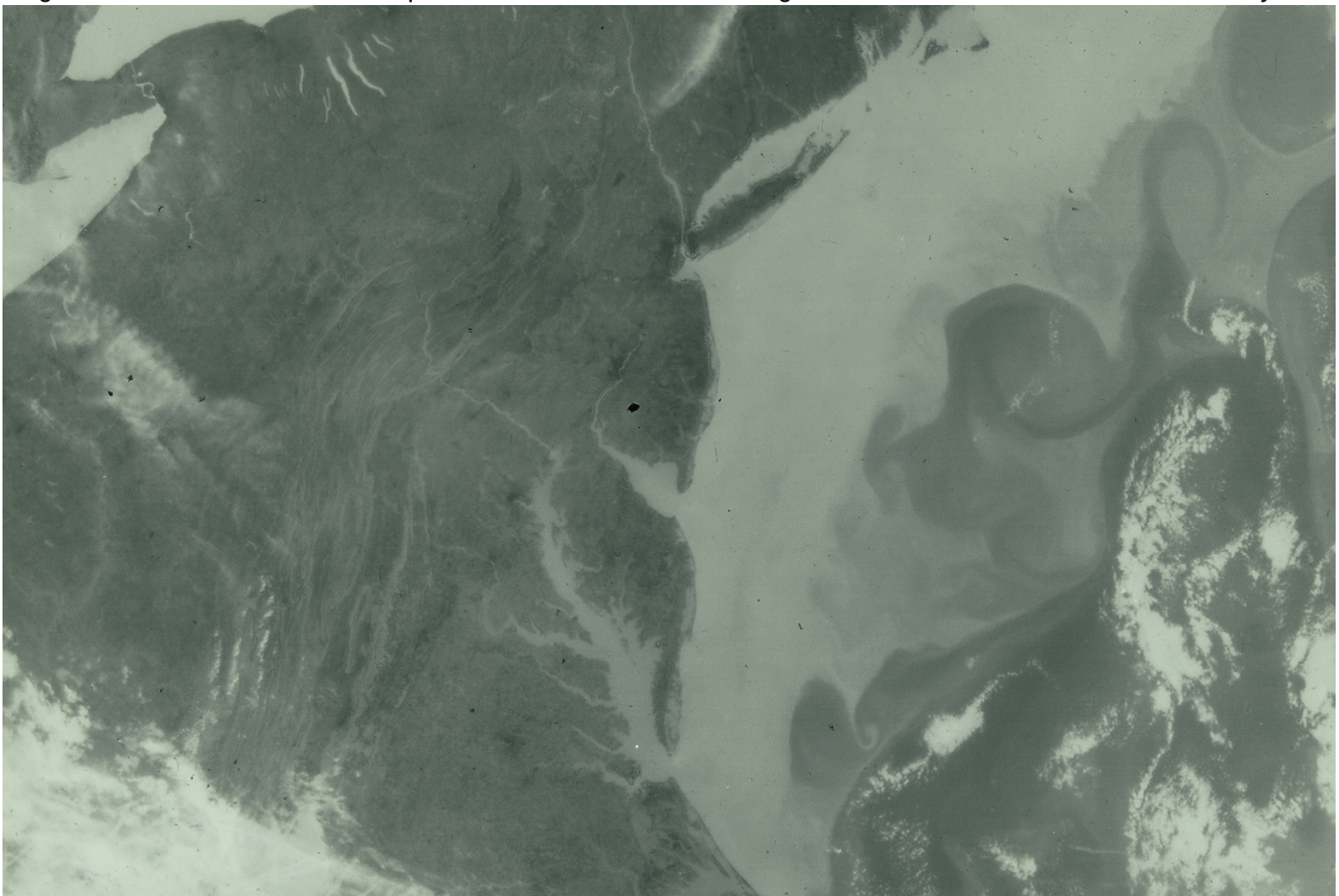

Fig. 13-2 Sea Surface Temperature - Analysis for Gulf Stream, May 1-4, 1977

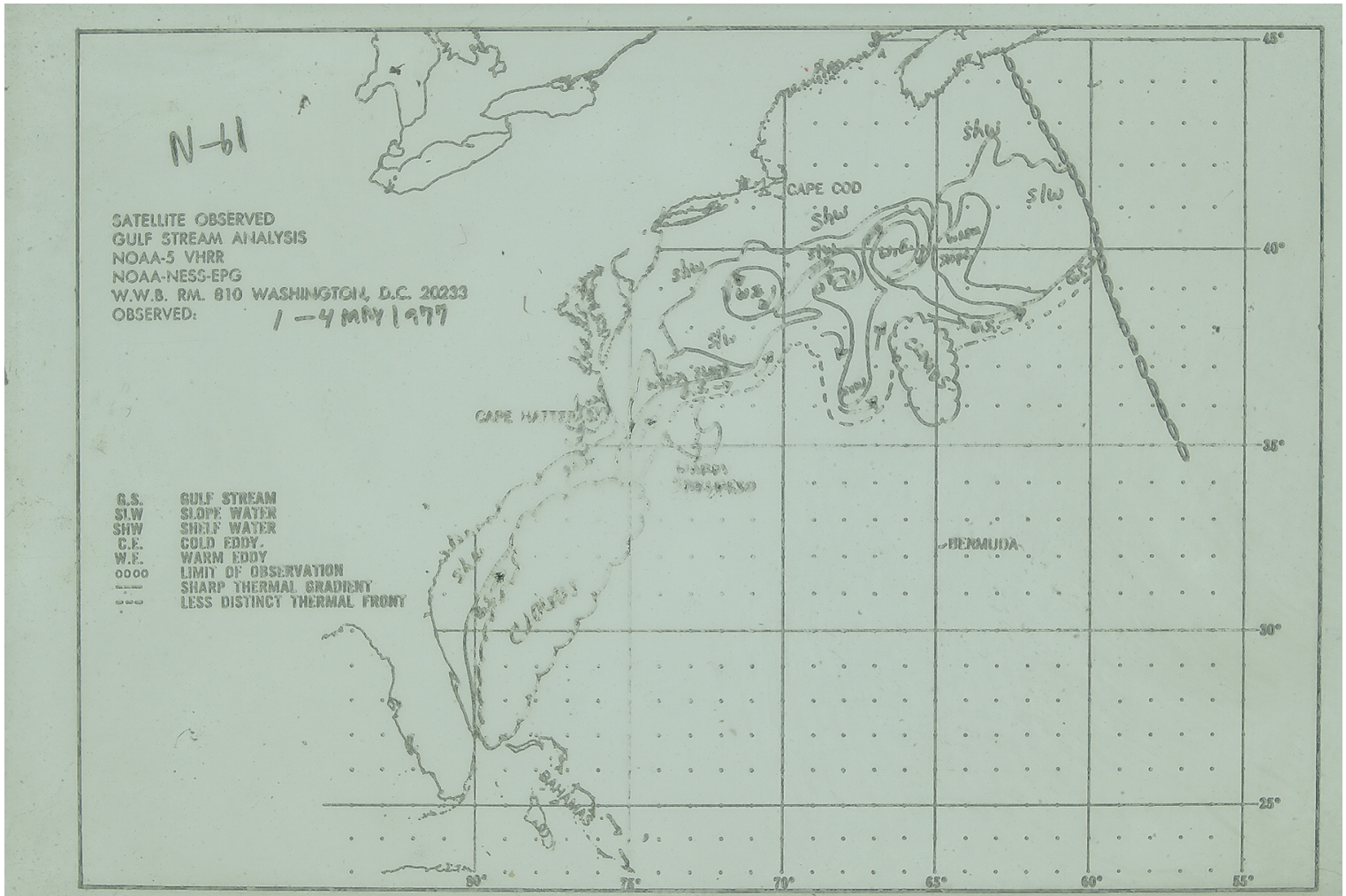

Fig. 13-3 West Coast Upwelling, September 11, 1974

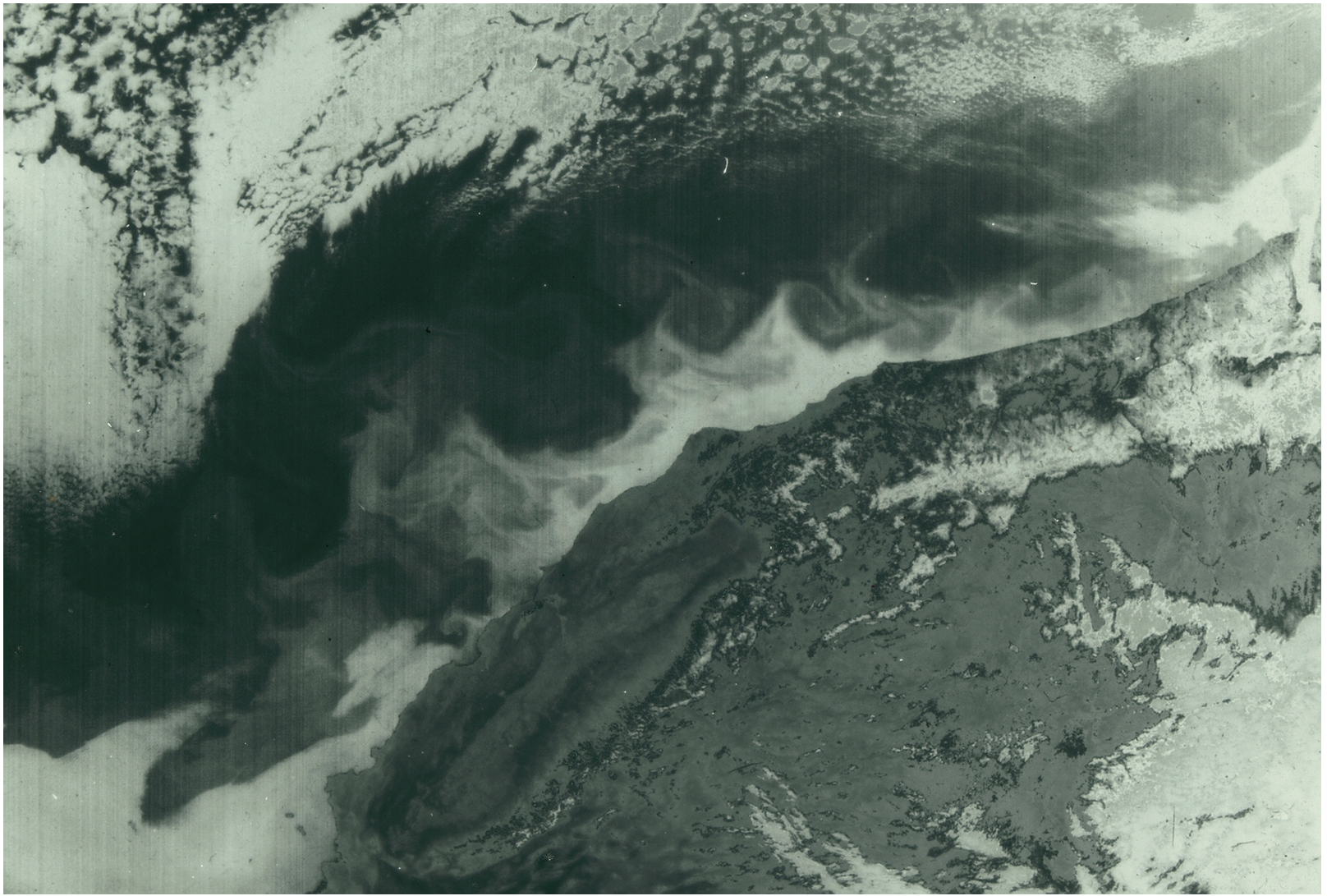

Fig. 13-4 AVHRR 4 vs. 5 Channel Algorithms

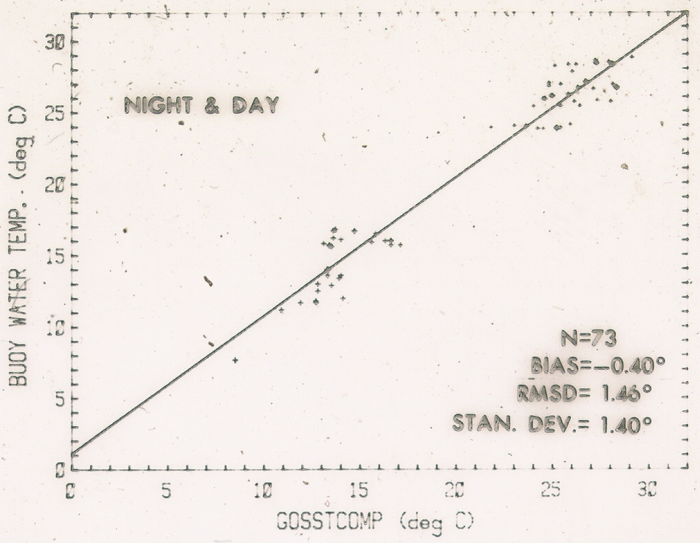

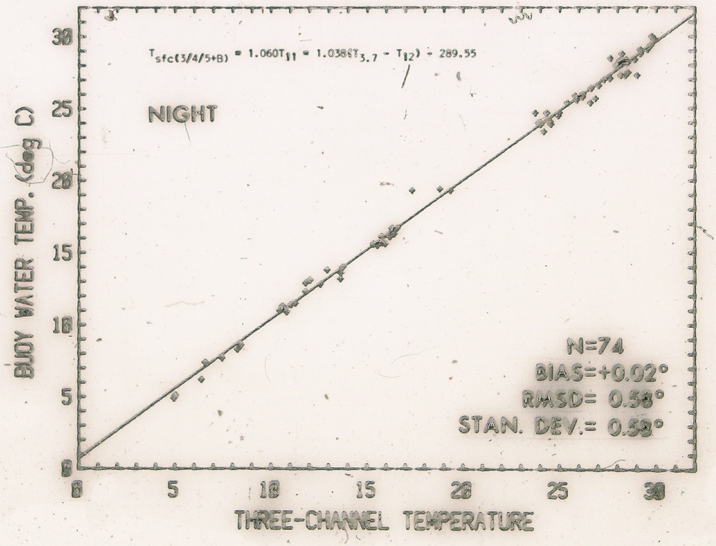

Fig. 13-5 Old vs. New Algorithms - Oct. vs. Nov. 1981

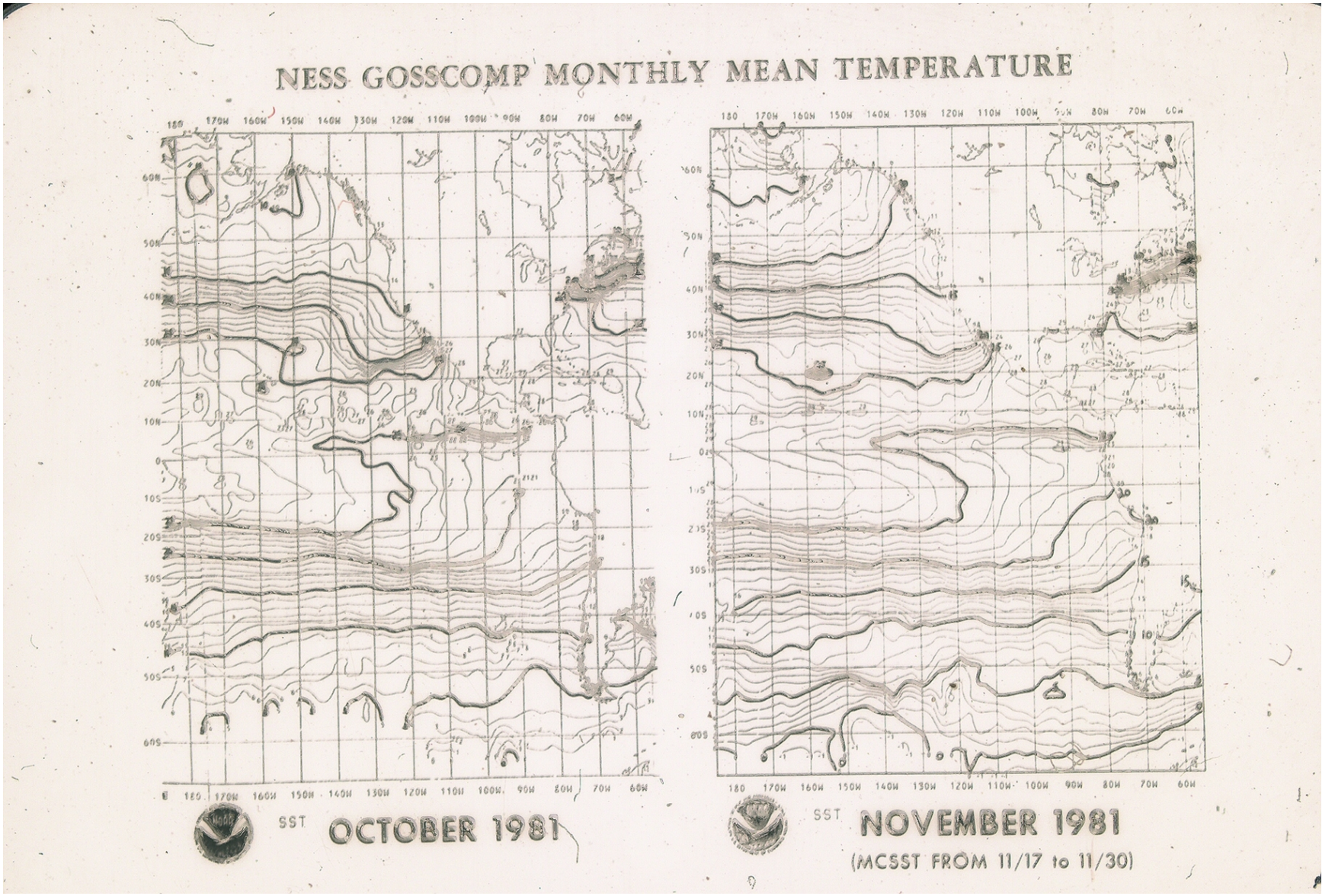

Fig. 13-6 Cloud Filtering Using 48 IR Images in 24 Hours - Gulf of Mexico

Fig. 13-7 Using VAS 3.9, 11 & 12.7 channels. Similar to AVHRR but lower resolution.

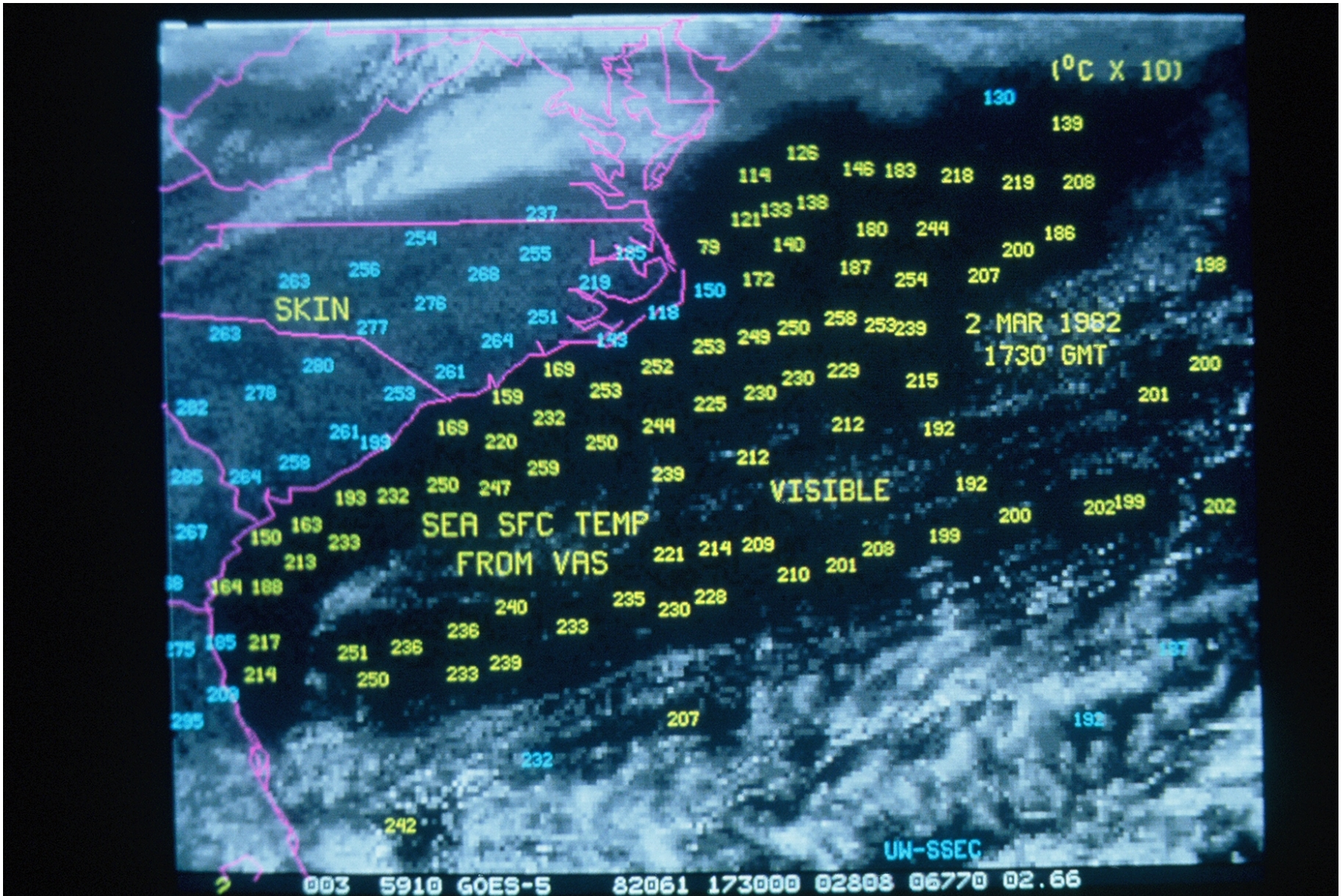

D. Scanning Multi-channel Microwave Radiometer (SMMR)
Flown on SEASAT and Nimbus-7. (Info courtesy of Wilheit, GSFC)
(unlabeled) Figure 13-8) - A. Shows relative response in microwave region to variation in different parameters. Point out frequencies of SMMR & resolution.
B. Presents accuracy of SST determinations.

III. Surface wind (or wind stress) - All Seasat obs. (3 mos., summer 1978)
A. Altimeter (speed only, at nadir beneath satellite)
$\sigma \sim .2$ to 2.5 mps up to 15 mps.
B. Scatterometer (speed and direction)
$\sigma \sim 1.5$ mps for speed and 20° direction from 2 to 25 mps. (upper limit of ground truth)

✓ - Figure 13-9 (slide): Processed scatterometer winds on TIROS N image {OFF E. COAST OF U.S. 11 SEPT. '78
Intense storm not predicted; white dots = ship observations.
QE II damaged; encountered >60 kt winds + waves > 15 M.

✓ - Figure 13-10 (slide): Typhoon Wendy, E. China Sea, 1056 GMT 30 July 1978.
line length proportional to speed.
Ambiguities not removed; up to 4 vectors per point. MAX. recorded = 35 MPS

IV. Significant wave Height from Seasat Altimeter ($H_{1/3}$)
✓ - Figure 13-11 (slide): compared to buoys, accuracy: Mean = 0.07 M; σ = 0.3 M RANGE = 0-10 M

V. Ocean currents and BOTTOM TOPOGRAPHY - Altimeter
Seasat precision: σ = 8 cm. [Accuracy depends on accuracy of satellite orbit + knowledge of the mean geoid of the earth.)
✓ - Figure 13-12 (slide): Orbit cross-section, 10 July 1978 (Departure from GEM10B mean geoid.)
• Effect of bottom topography, e.g., Puerto Rico Trench, Continental rise.
• Effect of currents: Gulf Stream, warm core eddy.

VI. Synthetic Aperture Radar (SAR) sea surface images (SEASAT)
Resolution ≐ 25 to 40 meters (depending on angle + processing)
✓ - Figure 13-13 (slide): Off Baja Calif (Mexico): Wind shadows of islands; internal waves (?)
✓ - Figure 13-14 (slide): Gulf of California: Top-tidal rips; center-internal waves. (?)

VII. Ocean Color Observations, Nimbus 7 Coastal Zone Color
A. Scanner (CZCS), Vis: .443, .520, .550, .670, .750 μm; IR = 10.5-12.5 μm
Scans ± 39° of nadir; resolution at nadir = 825 meters.
Phytoplankton (chlorophyll); Sediment + some pollution (not oil).

SCANNING MULTI-CHANNEL MICROWAVE RADIOMETER (SMMR) - SEASAT & NIMBUS-7

A. SCHEMATIC REPRESENTATION OF MICROWAVE SPECTRA OF VARIOUS PARAMETERS, P_i

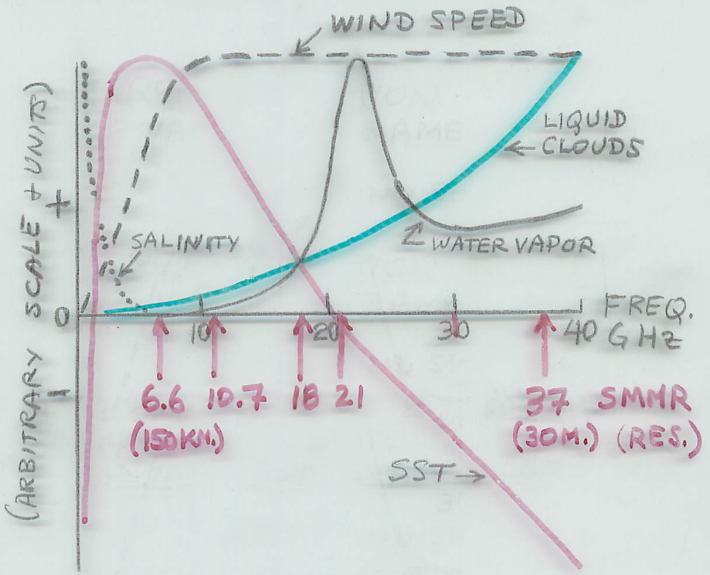

B. SMMR SST ALGORITHM RESULTS

COMPARISON DATA SOURCE	NUMBER OF OBS.	STANDARD DEVIATION ORIGINAL	STANDARD DEVIATION REVISED
CLIMATOLOGY	57,351	1.6°C	1.4°C.
SHIPS	23,267	1.7°C.	1.6°C.

Figure 13-8

From Wilheit, GLAS/GSFC/NASA

Fig. 13-9 Processed Scatterometer Winds on TIROS-N - off E. Coast of U.S. Sept. 11, 1978

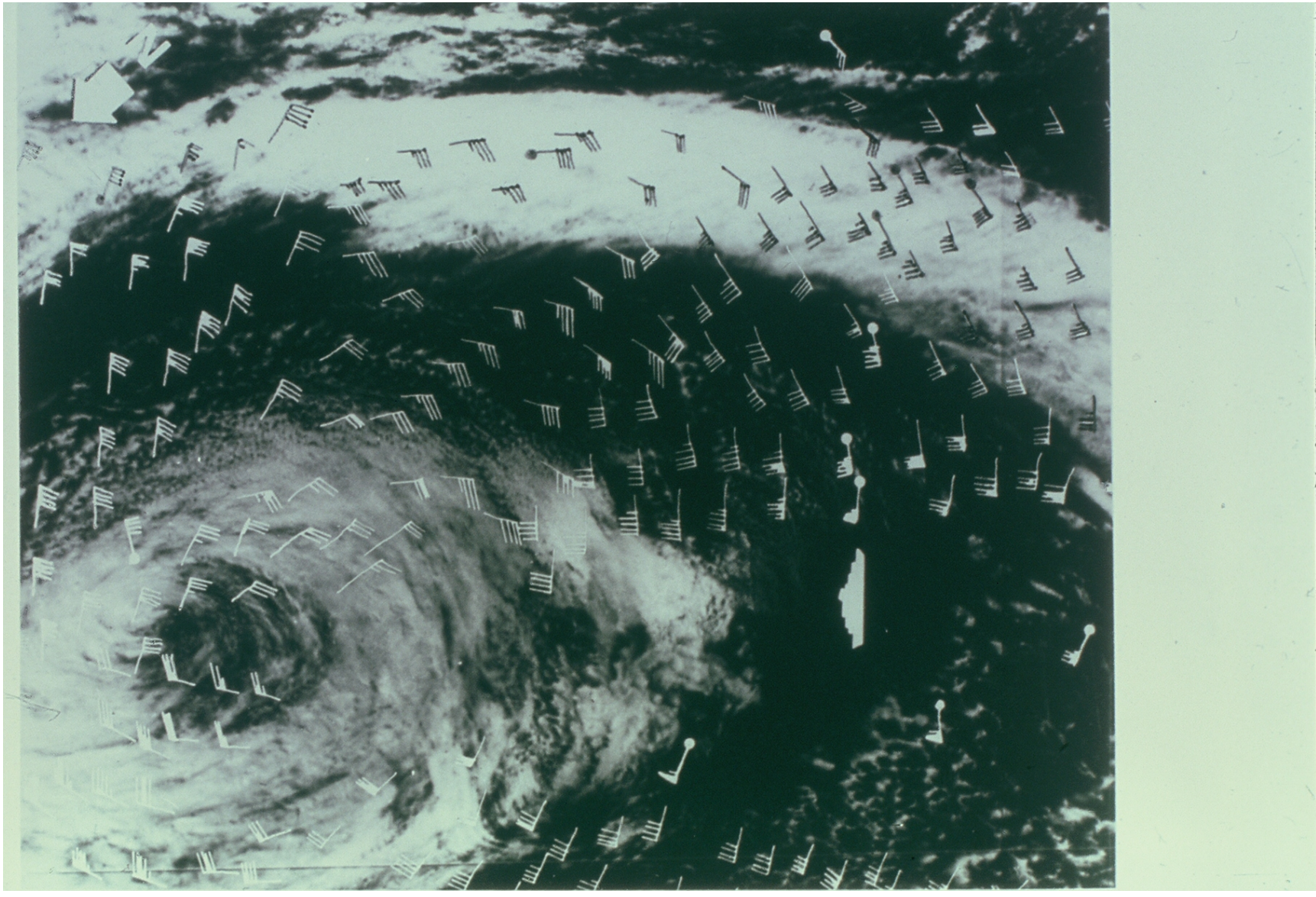

QE II Damaged

Fig. 13-10 Typhoon Wendy, E. China Sea, July 30, 1978

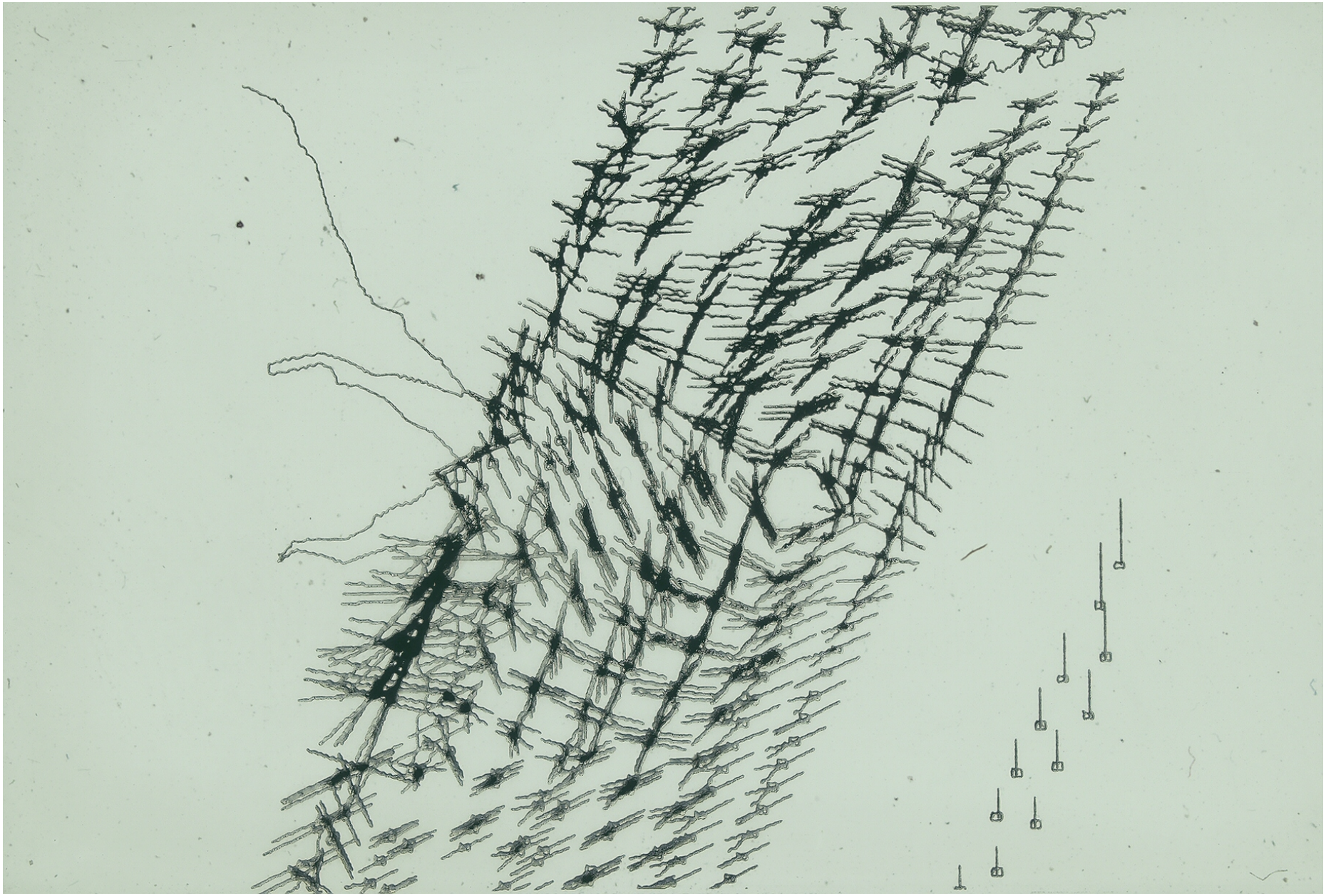

Fig. 13-11 Significant Wave Height from Seasat Altimeter

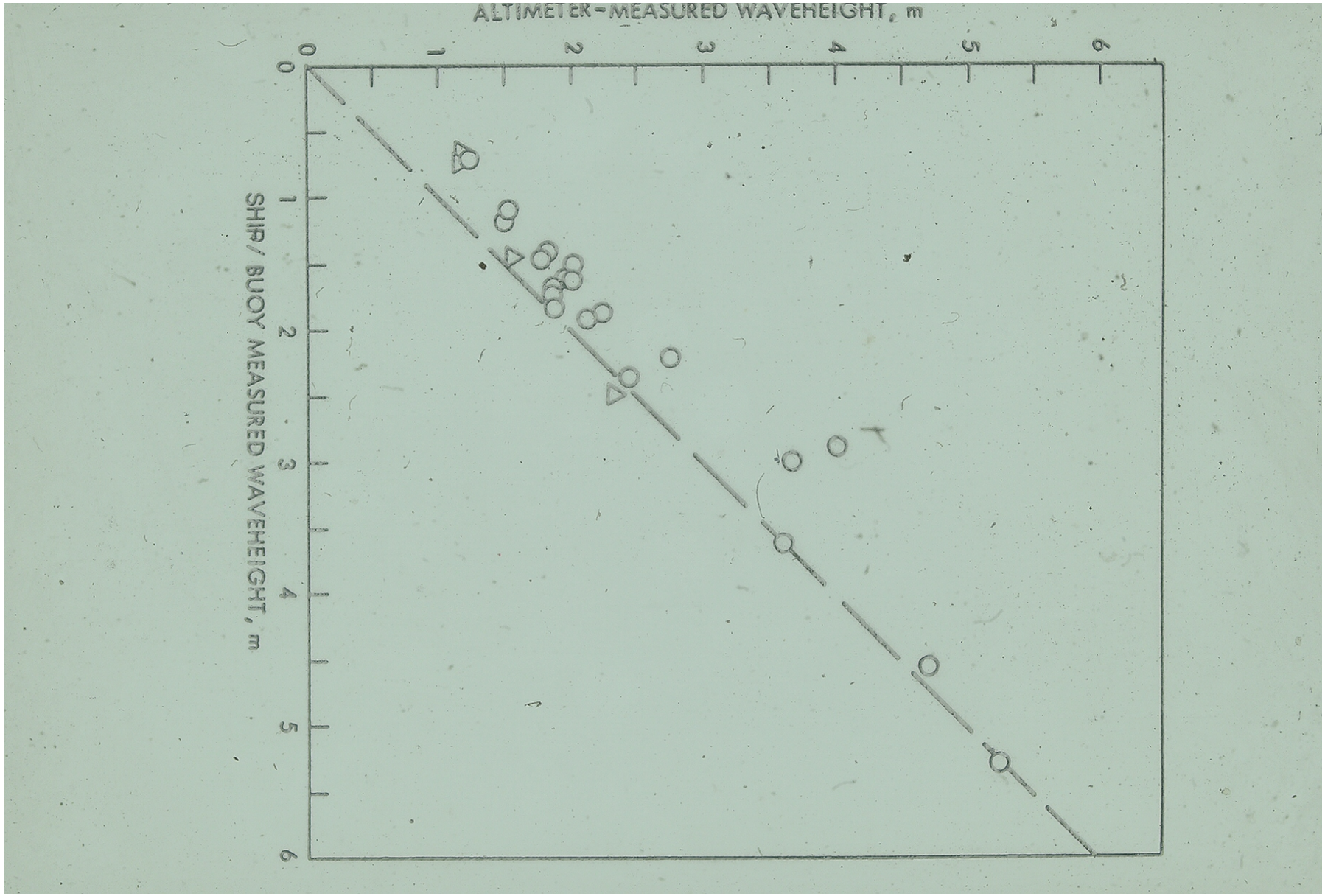

Fig. 13-12 Seasat Altimeter Orbit Cross-Section, July 10, 1978

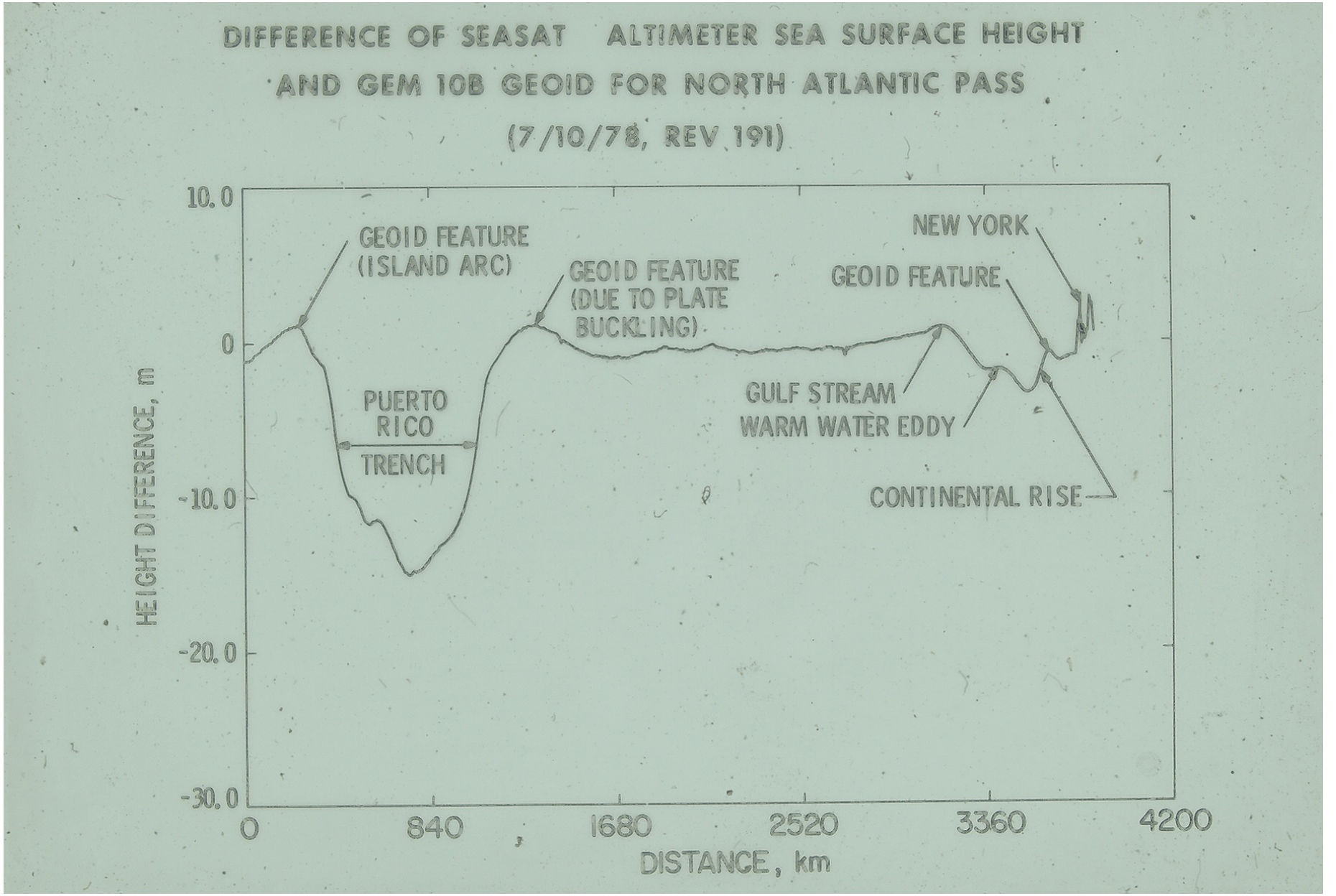

Fig. 13-13 Seasat SAR - Off Baja, CA
Synthetic Aperture Radar (SAR) Sea Surface Images (Seasat)

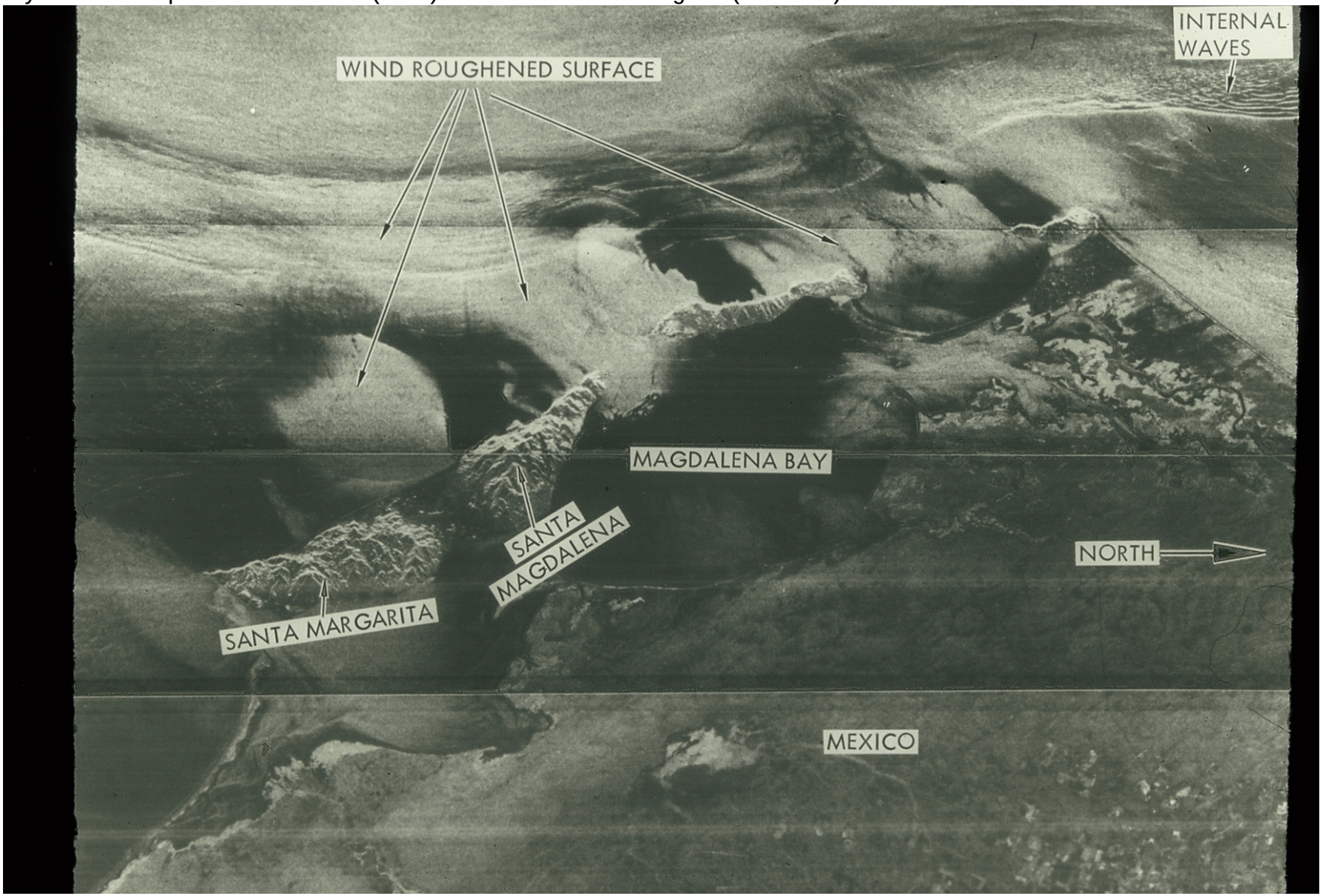

Fig. 13-14 Seasat SAR - Gulf of Claifornia - Top Tidal Rips

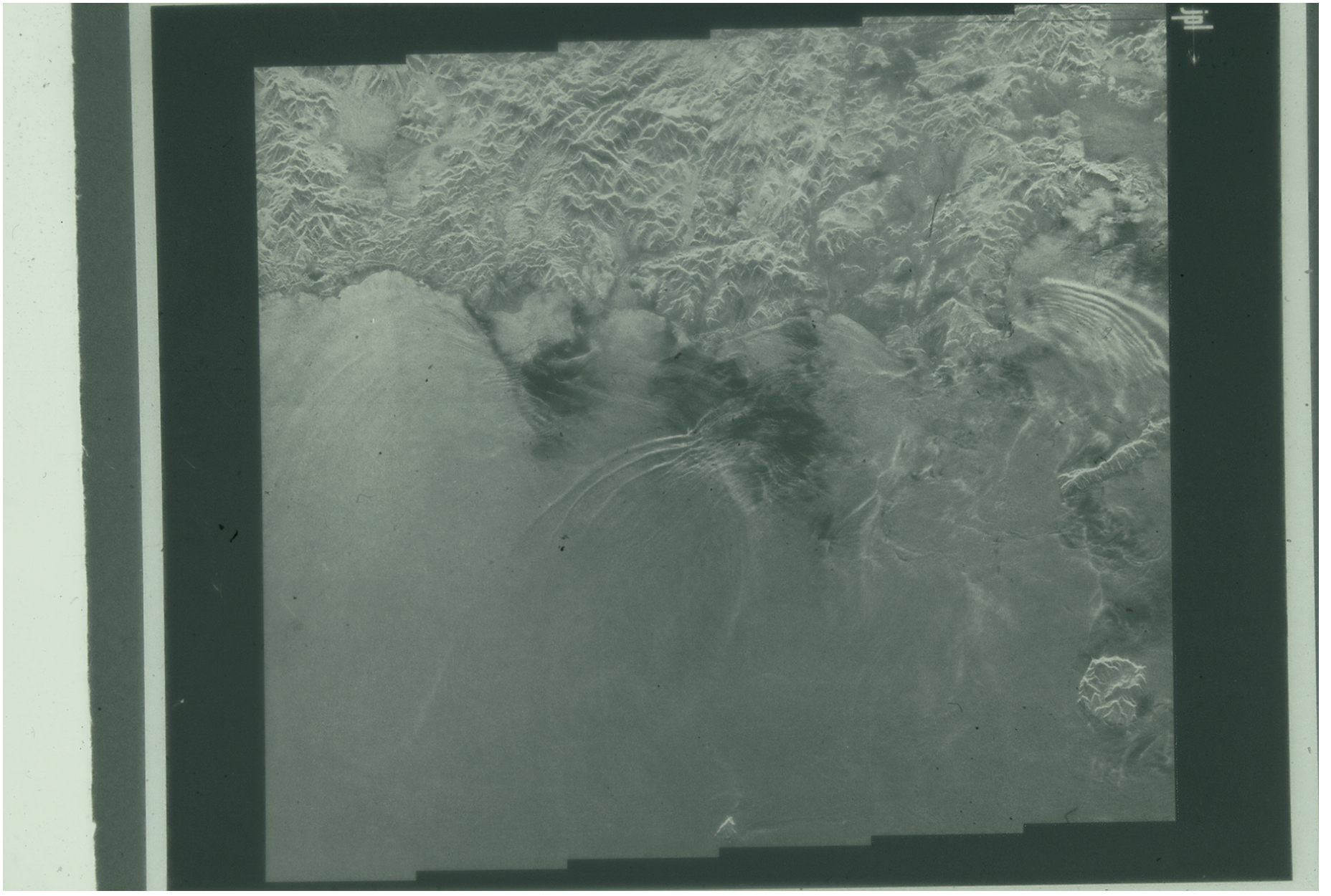

B. Must carefully correct each channel for atmospheric scattering & absorption of solar radiance to retrieve the radiance in each visible channel scattered by the water mass. Processing technique allows latter to be determined with error ~ 10%.

(*) Pass print around room: Top is atmospheric correction (attenuation coefficient); bottom is pigment concentration. Land + clouds are black.

- Figure 13-15 (vu-graph) — (Left with PRC): Unprocessed data: BO HAI, KOREA BAY, N. YELLOW SEA 11 Feb. 1980.
  Data archived in this form & on magnetic tape.
  More Atmos. scattering at shorter wavelengths. { 0.4 μm = 2 X that at 0.7 μm
  Little water penetration at longer wavelengths.
  Pigment strongly absorbs at 0.443 μm, thus the more pigment the blacker the image (lower radiation)
  Pigment weakly absorbs at 0.520 & 0.550 μm, so the image is lighter (more radiation due to more backscattered sun light)
- Figure 13-16 (vu-graph) — (left with PRC): Same, but 16 Feb. 1980; Look at difference in patterns.

C. Calculation of pigment concentration (phytoplankton — bottom of the fish food chain. = chlorophyl a (~90%) + phao-pigments a (~10%) → dead material). Two algorithms:

$$\text{Low } C = 0.5\left(\frac{R_{.443}}{R_{.550}}\right)^{-1.3} \quad (0.05 - 1.0\ mg/m^3) \qquad \text{High } C = 0.8\left(\frac{R_{.520}}{R_{.550}}\right)^{-4.0} \quad (0.1 - 10.\ mg/m^3)$$

{ corrected for atmosphere.

- Improved, more complicated algorithms: See Gordon, H.R., et al, Applied Optics, V.22, pp. 20-36 (1 JAN. 1983).
- Estimated pigment concentrations agree within 30-40% of measured values; ship observations considered of similar accuracy.

✓ - Figure 13-17 (slide): Low pigment concentration, 14 June 1979.
  Coastal waters with high pigment concent., saturated
  Shows variations off-shore; effect of Gulf Stream.

✓ - Figure 13-18 (slide): Thermal channel of CZCS - High correlation with pigment concentration.
  (See slide = Figure 8-3)

Fig. 13-15 and Fig. 13-16 Vu-graphs

Unprocessed Data – left with PRC

Bo Hai, Korea Bay, N. Yellow Sea – February 11, 1980 and February 16, 1980

Fig. 13-17 Phytoplankton Pigments - Low Concentration, June 14, 1979

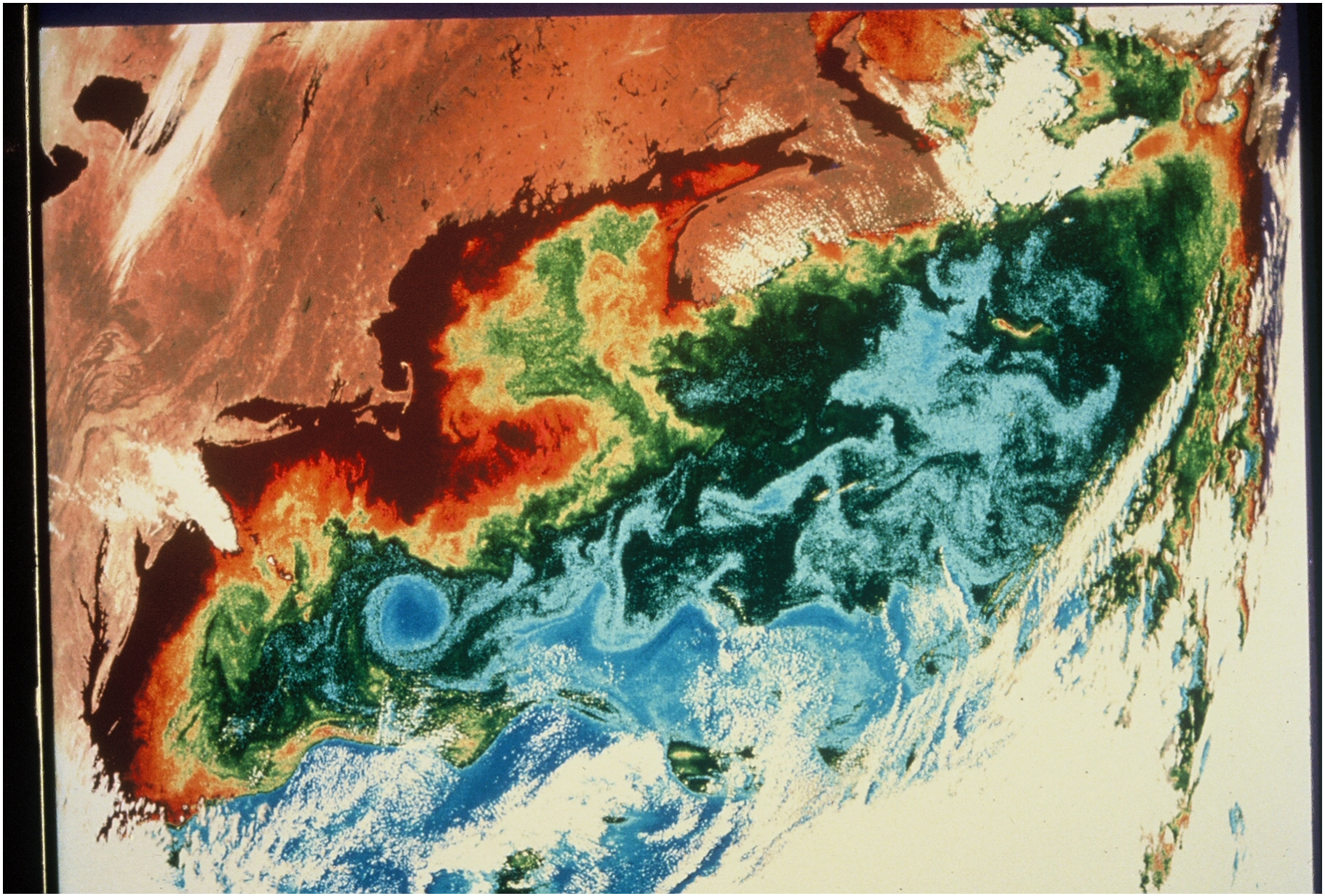

Fig. 13-18 Thermal Channel of CZCS;high correlation with pigment concentration

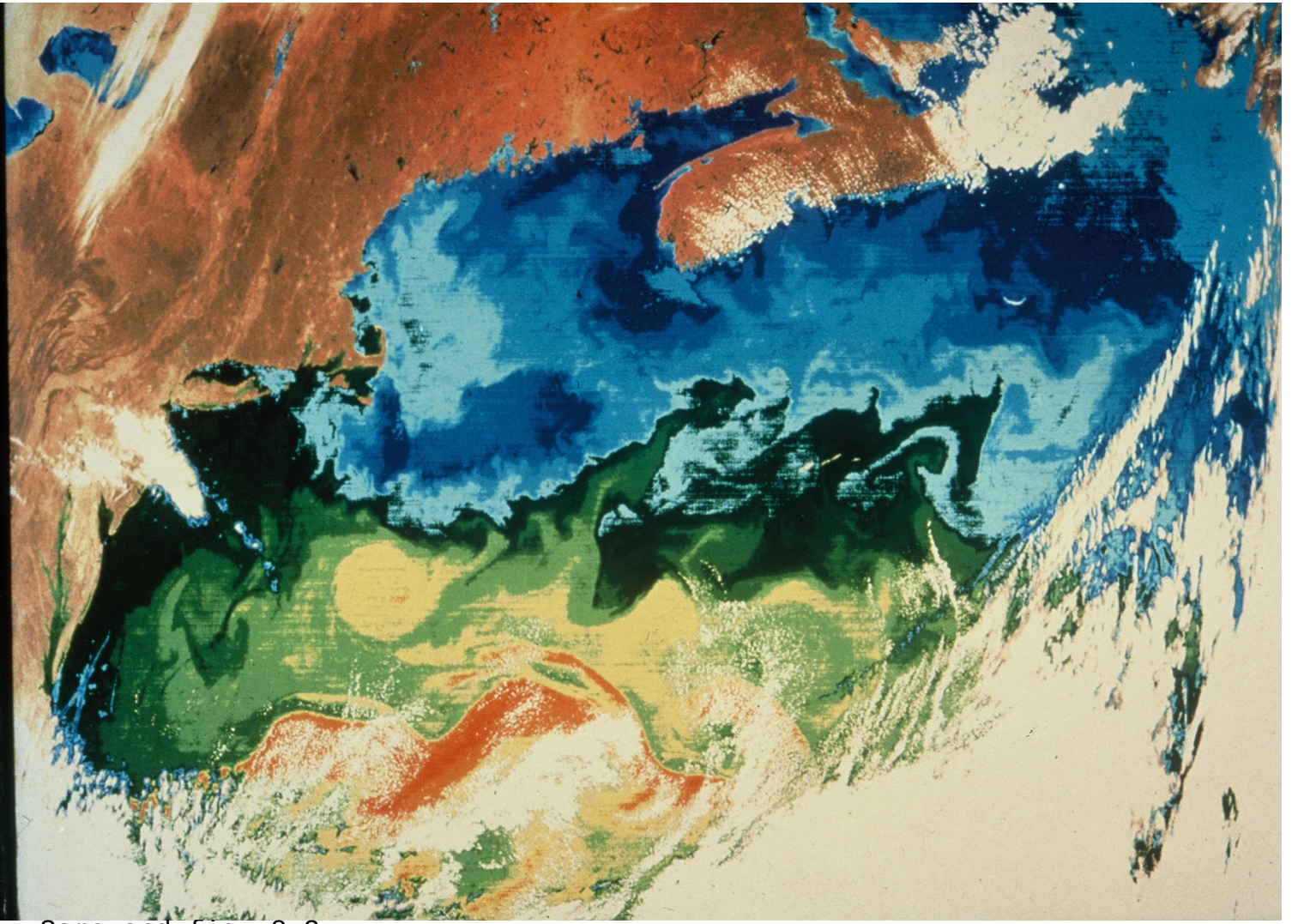

Same and fig. 8-3

✓ - Figure 13-19 (slide): High pigment concentration - Shows variations in coastal waters, but loose details off-shore. Georges Bank off Cape Cod is yellow.

✓ - Figure 13-20 (slide): Gulf of Mexico, 13 Nov. 1978. Low pigment concentration - Water W. of Florida saturated because of high concentration there.

✓ - Figure 13-21 (slide): High concentration presentation. Track of oceanographic ship Athena off Florida Coast through high concentration area superimposed.

✓ - Figure 13-22 (slide): Comparison of (high) pigment concentrations along the track, by ship observations & satellite determination.

D. Sediment and Pollution.

- Determination of pigment concentration is complicated by presence of heavy pollution or sediment in the surface waters. But CZCS ~~may~~ can be helpful in locating and identifying sources and tracks of such pollution and sediment.

✓ - Figure 13-23 (slide): Example of pollution, using Channels 1, 2 & 3. Shows dump of sewage off the east coast of the U.S.A. (light gray area) (27 August 1979.) Unfortunately, previous dumps are drifting SSW toward swimming beaches on the Virginia coast! (Cannot detect oil slicks.)

VIII. Outlook for ocean observations.

- No operational commitments other than sea surface temperature.
- ESA's ERS-1 similar to SEASAT; Japan working on microwave sensors.
- GRAUSAT (Altimeter only; operational wind speed extraction)
- Proposed TOPEX (USA-France Altimeter + Scatterometer); Proposed NROSS (USA - "Poor man's SEASAT)

Fig. 13-19 Phytoplankton Pigments - Low Concentration, June 14, 1979

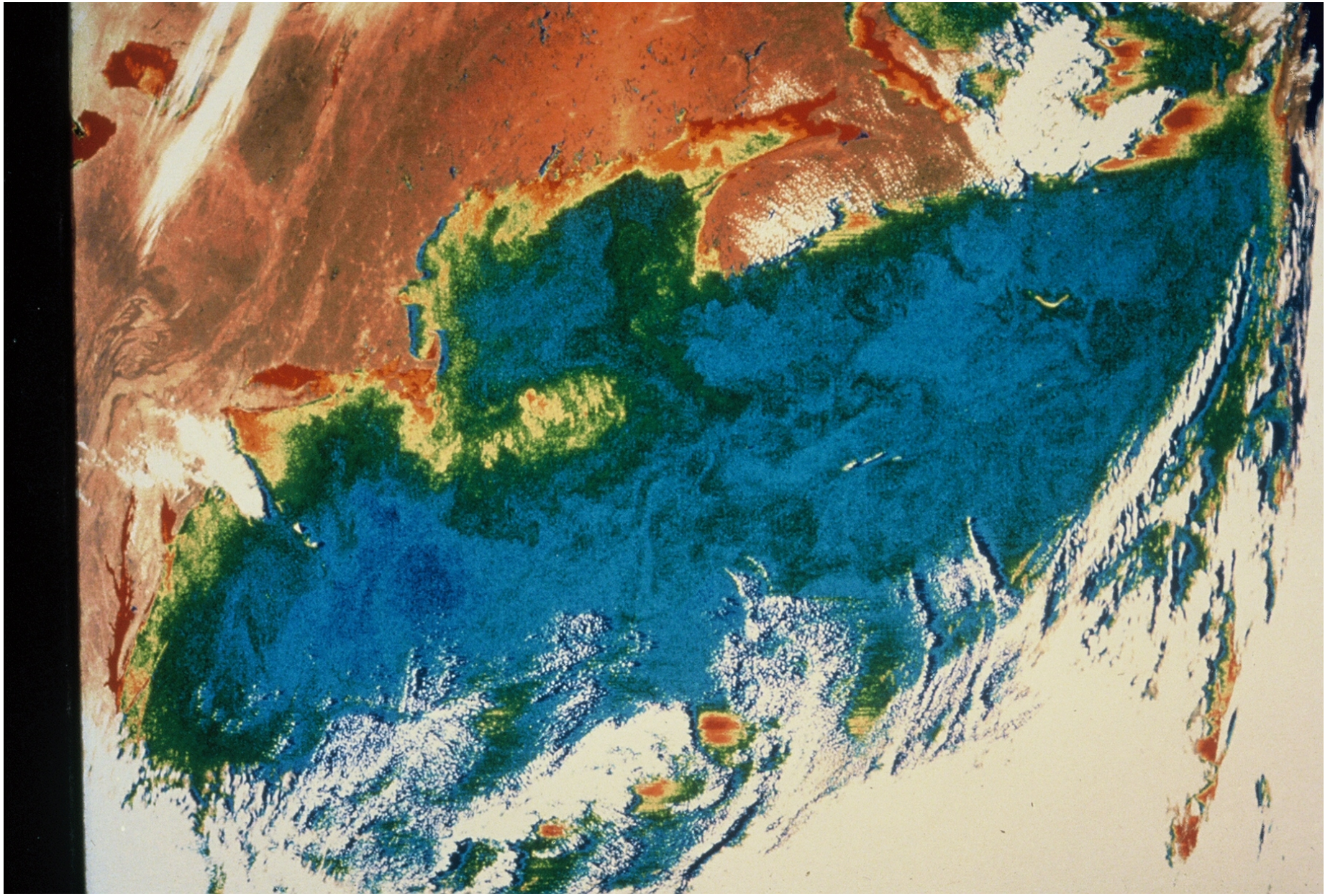

Fig. 13-20 Gulf of Mexico

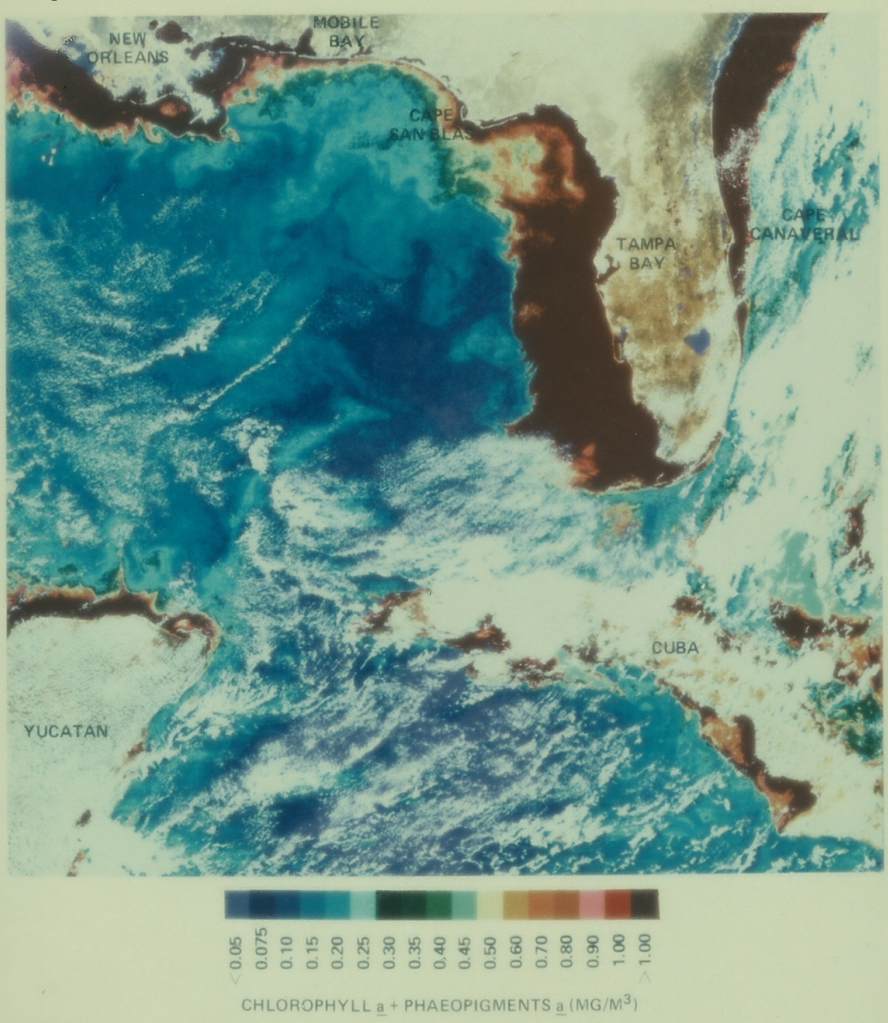

Low Pigment Concentration

Fig. 13-21 High Concentration

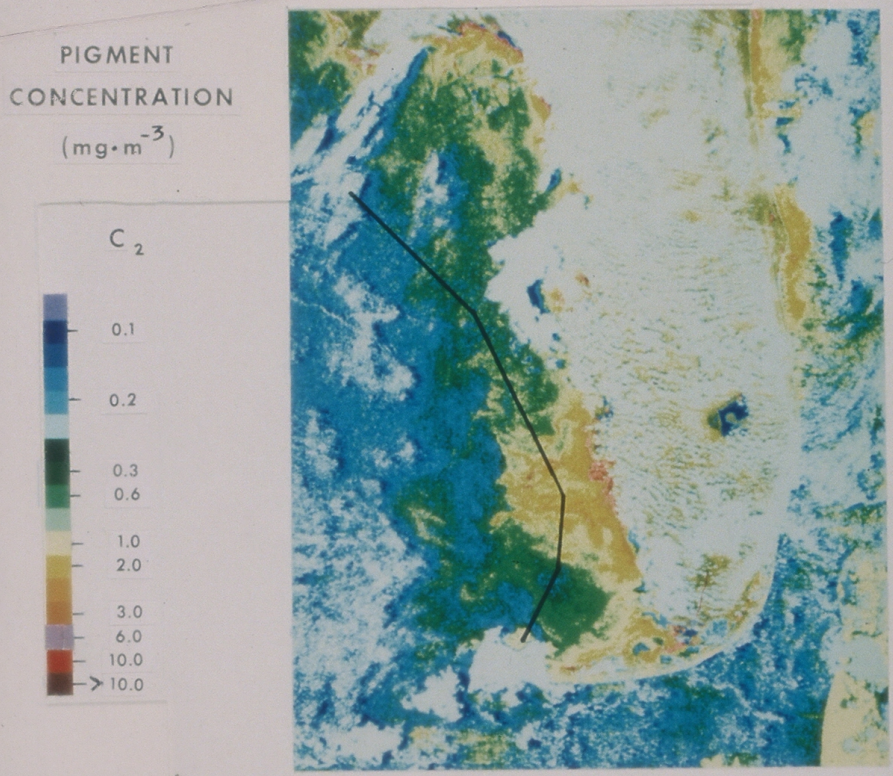

$$C_2 = 0.8 \left(\frac{L_{520}}{L_{550}} \right)^{-4.0}$$

Track of Oceanographic Ship Athena off Florida - November 13, 1978

Fig. 13-22 Comparisons of high pigment concentrations along of track, by ship observations and satellite determination

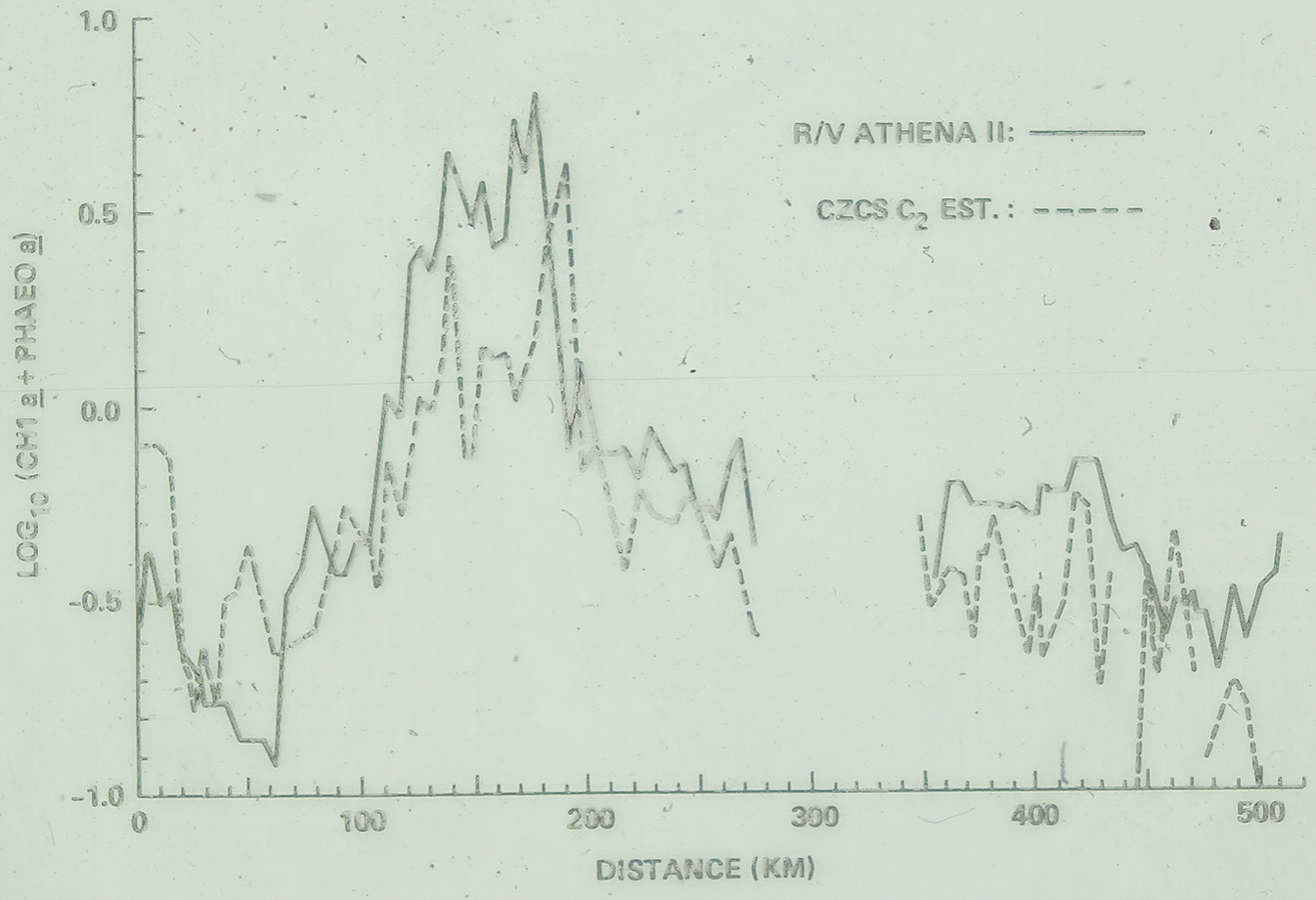
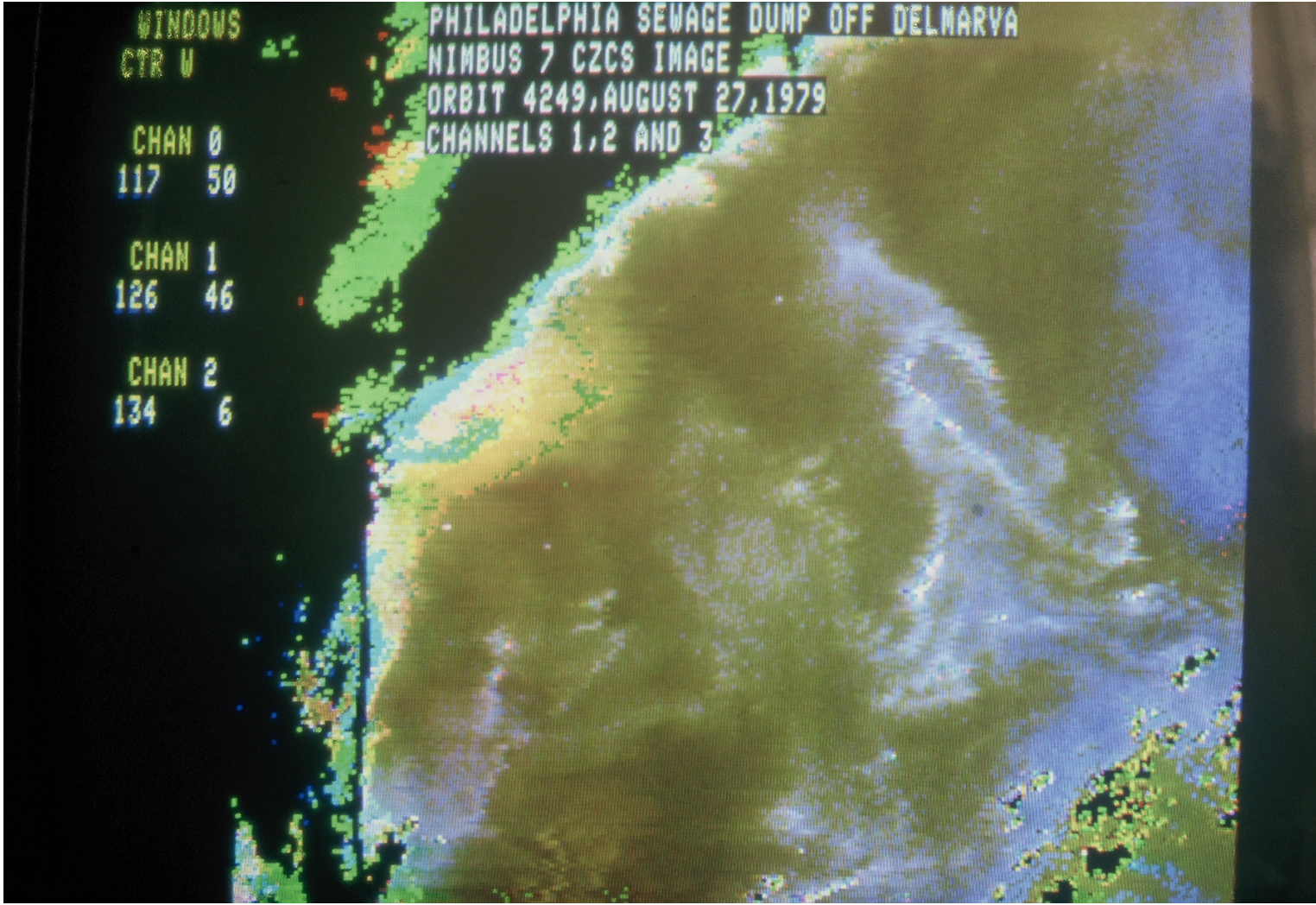
Fig. 13-23 Example of Pollution; Sewage Dump Off DELMARVA - August 27, 1979